BIODIVERSITAS
Volume 26, Number 7, July 2025
Pages: 3600-3609

ISSN: 1412-033X
E-ISSN: 2085-4722
DOI: 10.13057/biodiv/d260746

Metabolomic profiling and antifungal potential of turmeric (*Curcuma longa*) root exudate against *Ganoderma boninense*

LIDYA KARLINA[1], SUWANDI SUWANDI[1,2,♥], RAHMAD FADLI[2], A. MUSLIM[2], HARMAN HAMIDSON[1,2], CHANDRA IRSAN[1,2]

[1]Graduate Program of Plant Sciences, Faculty of Agriculture, Universitas Sriwijaya. Jl. Padang Selasa No. 524, Palembang 30139, South Sumatra, Indonesia
[2]Department of Plant Protection, Faculty of Agriculture, Universitas Sriwijaya. Jl. Raya Palembang-Prabumulih Km 32, Ogan Ilir 30662, South Sumatra, Indonesia. Tel.: +62-711-580059, Fax.: +62-711-580276, ♥email: suwandi@fp.unsri.ac.id

Manuscript received: 25 March 2025. Revision accepted: 30 July 2025.

Abstract. *Karlina L, Suwandi S, Fadli R, Muslim A, Hamidson H, Irsan C. 2025. Metabolomic profiling and antifungal potential of turmeric* (Curcuma longa) *root exudate against* Ganoderma boninense. *Biodiversitas 26: 3600-3609. Ganoderma boninense*, the causative agent of basal stem rot, significantly threatens oil palm cultivation. Turmeric (*Curcuma longa*) is a potential source of antifungal compounds for agricultural applications. This study investigates the antifungal properties of root exudates from four turmeric ecotypes (Palembang, Bandung, Surabaya, and Bangka) against *Ganoderma boninense* and employs untargeted metabolomics using LC-HRMS. The root exudates were collected from two-month-old plants grown in soil by incubating the roots in aerated sterile distilled water for 12 hours. The exudates were then filter-sterilized and directly used for antifungal assays and metabolomic analysis. The results revealed that turmeric root exudates at concentrations of 1.25%, 5%, and 20% inhibited *G. boninense* growth in a concentration-dependent manner, with the efficacy varying depending on turmeric ecotypes. The Palembang ecotype exhibited the strongest antifungal activity, with inhibition rates of 37.7% to 46.7%. The Bandung and Surabaya ecotypes showed moderate inhibition (10.3-36.2%), while the Bangka ecotype had weak effects. None of the turmeric exudates at concentrations between 1.25% and 20% promoted the growth of *G. boninense*. Metabolomic profiling played a crucial role in this study, identifying 193 metabolites, with 20 significant differentially accumulated metabolites in the inhibitory exudate group. Key metabolites such as azelaic acid, bis(2-ethylhexyl) phthalate, haplofungin C, menthyl acetate, and piptamine were identified, shedding light on their potential contribution to antifungal activity. These findings indicate that turmeric root exudates contain bioactive compounds that could be explored as eco-friendly biocontrol agents against *G. boninense*.

Keywords: Antifungal activity, bioactive root exudate, *Curcuma longa*, metabolomics, oil palm basal stem rot

INTRODUCTION

Ganoderma boninense is a significant pathogen that causes Basal Stem Rot (BSR) in oil palm (*Elaeis guineensis* Jacq.), providing a major threat to the oil palm industry, particularly in Southeast Asia. The disease was first recognized in the 1960s and has caused significant economic losses, with reports indicating yield reductions of up to 50-80% in severely affected plantations (Kamu et al. 2021). Typical symptoms of BSR include yellowing of leaves, failure of young leaves to open, and the presence of fruiting bodies of *G. boninense* at the base of the stem (Khoo and Chong 2023). These symptoms indicate severe damage to the palm vascular system, restricting water uptake and eventually leading to plant death (Zakaria 2023). BSR spread rapidly in replanting areas and converted lands, resulting in alarmingly high infection rates in newly established plantations (Priwiratama et al. 2020). The pathogen prevalence has been documented across various soil types, including mineral and peat soils, highlighting its adaptability and the challenges it creates in oil palm cultivation (Ibrahim et al. 2020; Virdiana et al. 2024). This adaptability is further evidenced by the ability of the pathogen to infect oil palm at all growth stages, from seedlings to mature trees, which complicates management strategies (Khoo and Chong 2023).

Perennial allelopathic herb plants show potential as protective agents against chronic diseases, such as *Ganoderma*. Intercropping with taro plants has been demonstrated to inhibit infections and to reduce the inoculum potential of *G. boninense* in oil palm (Suwandi et al. 2024). Specifically, intercropping with ginger (*Zingiber officinale*) and Java turmeric (*Curcuma xanthorrhiza*) has been shown to reduce *G. boninense* infections in oil palm (Suwandi et al. 2023). The suppression of *Ganoderma* in oil palms intercropped with these rhizomatous herbs is a result of a complex and fascinating interaction. The antifungal properties of their root exudates, which are complex organic compounds released into the rhizosphere, play a crucial role in this process. These exudates shape the microbial community and influence soil microorganisms, including phytopathogenic fungi, through a variety of compounds such as carbohydrates, organic acids, amino acids, and secondary metabolites that can stimulate or inhibit microbial populations (Sun et al. 2023). These exudates serve as a food source and signaling molecules for microorganisms, influencing their recruitment, growth, and community structure. This interaction is essential for plant health, as beneficial microbes aid in nutrient uptake, disease resistance, and overall plant growth (Gu et al. 2024).

Certain root exudates exhibit significant antifungal effects on specific phytopathogenic fungi. For instance, ethyl acetate extract of root exudates from perennial herbaceous plants, *Canna indica* and *Xanthosoma sagittifolium*, has been shown to reduce the growth of *G. boninense* (Suwandi et al. 2022). Root exudates from wheat contain phytosphingosine that directly inhibit *Fusarium oxysporum* f. sp. *niveum* and modify the watermelon rhizosphere microbiome, thereby suppressing pathogen invasion and reducing *Fusarium* wilt incidence in the wheat-watermelon intercropping system (Li et al. 2020). Root exudates from maize, barley, mung bean, chard, and sunflower contain phenolic and terpenoid compounds that inhibit the growth of pathogens such as *Rhizoctonia solani* and *Pythium ultimum* (Hussien and Abbas 2023). Root exudates from invasive plant *Wedelia trilobata* root exudates have antifungal properties against various soil-borne pathogens like *Rhizoctonia solani*, *Sclerotinia sclerotiorum*, and *Fusarium oxysporum* (Xiang et al. 2023). Peng et al. (2024) found that isoliquiritigenin and lauric acid have been identified as key antifungal compounds that are effective against *Phytophthora nicotianae*, the cause of tobacco black shank disease, in resistant tobacco root exudates. Recently, Wu et al. (2025) reported that jasmonic acid metabolism detected in the root exudates of resistant konjac cultivars is involved in the regulation of soft rot disease resistance.

Although the antifungal properties of turmeric rhizome extracts are well-known, the antifungal activity of its root exudates remains underexplored. Liquid Chromatography-High Resolution Mass Spectrometry (LC-HRMS) has proven to be a powerful and highly sensitive detection tool in metabolomics for identifying and characterizing bioactive compounds (de Souza et al. 2021; Triastuti et al. 2023). In the context of antifungal studies, LC-HRMS enables the comprehensive profiling of plant extracts, facilitating the identification of key metabolites involved in inhibiting pathogenic fungi (Lima et al. 2022). This research employed an exudate metabolomics approach with LC-HRMS to analyze upregulated and downregulated metabolites to identify compounds with antifungal properties. This study aimed to evaluate the antifungal potential of root exudates from different turmeric ecotypes against *G. boninense* and to identify key bioactive metabolites through untargeted metabolomic profiling.

MATERIALS AND METHODS

Plant materials and collection of root exudate

Turmeric rhizomes representing four local varieties or ecotypes were collected from local markets in Indonesia, namely: Kp from Palembang, South Sumatra; Bd from Bandung, West Java; Ks from Surabaya, East Java; and Bb from Bangka Island. First, the rhizomes were planted in a cocopeat medium until sprouting and then transferred to a compost medium in five-liter pots. The plants were fertilized biweekly with a fermented liquid cow manure compost extract. At the actively growing root stage (two months old), three plants with intact rhizomes were carefully uprooted at noon (5:00 p.m.) and gently rinsed under running tap water to remove any adhering soil. Any dead rhizomes or root parts were then removed. The plants, with intact roots and rhizomes, were weighed to approximately 250 g and immersed in 500 mL of sterile distilled water. The water was continuously aerated for 12 hours overnight to allow root and rhizome exudation into the water. The exudates were filtered twice: first through Whatman No.1 filter paper (GE Healthcare Bio-Sciences, Pittsburgh, PA, USA) and then using a 0.22-μm PVDF filter (Hawach Scientific, Xi'an, China) (Salem et al. 2022). The sterile filtered root exudates were defined as 100% concentration and stored at 4°C prior to use. A total of 19 root exudate samples were collected—five samples each from Kp, Bd, and Bn ecotypes, and four samples from the Ks ecotype. The turmeric cultivation was conducted in a greenhouse, and the root exudate extraction was carried out at the Laboratory of Phytopathology, Department of Plant Protection, Faculty of Agriculture, Universitas Sriwijaya, Indonesia. The experiment was conducted from January to December 2024.

Antifungal effect of root exudate on *Ganoderma boninense* growth

The inhibitory effect of root exudates on the mycelial growth of *G. boninense* was evaluated as follows. Different concentrations of root exudates (0%, 1.25%, 5%, and 20%) were prepared by diluting the exudates with sterile distilled water. For the 0% concentration (control), only sterile distilled water was added. Each concentration was mixed with molten MEA and poured into 90-mm Petri dishes. Five-millimeter mycelium-containing agar plugs from five-day-old MEA cultures were placed at the center of the dishes and incubated at 28°C in the dark. Colony diameter was measured daily until the control reached the edge of the plate. Fungal growth was observed based on colony diameter, and the Radial Growth Rate (RGR) was expressed as the mycelial growth rate (mm/day); this was determined from the slope of the linear regression between colony radius (y-axis) and days of incubation (x-axis) (Upasani et al. 2016). The experiment was conducted with five replications. The inhibition of *Ganoderma* RGR by root exudates was calculated using the following formula: [(RGR of control plate - RGR of treated plate)/RGR of control plate] × 100%. The RGR inhibition was reported as either the average or maximum inhibition for each root concentration.

Metabolomic study of root exudate

Ten root exudates with varying antifungal activities were selected for metabolomic analysis. Four exudates representing the Palembang and Bandung ecotypes, which showed significant RGR inhibition of *G. boninense* across the tested concentration (Kp-4, Kp-5, Bd-2, and Bd-3), were attributed to inhibitory exudate (IE group). Meanwhile, six exudates with no significant RGR inhibition (Ks-1, Bn-1, Bn-2, Bn-3, Bn-4, and Bn-5) were classified as non-inhibitory exudate (NIE group) (Figures 1 and 2). These samples were transferred to the LC-HRMS laboratory for metabolomic analysis. A 500-µL sample was diluted with 500 µL HPLC-grade methanol, vortexed for 1 minute, sonicated for 30 seconds, and centrifuged for 5 minutes at 1400 × g. The supernatant was filtered using a 0.2-µm nylon filter.

Liquid chromatography was performed using a Thermo Scientific™ Vanquish™ UHPLC Binary Pump, and mass spectrometric analysis was conducted using a Thermo Scientific™ Q Exactive™ Hybrid Quadrupole-Orbitrap™ Mass Spectrometer. A Thermo Scientific™ Accucore™ Phenyl-Hexyl column (100 mm × 2.1 mm ID × 2.6 µm particle size) was utilized for chromatographic separation. Mobile phases consisted of MS-grade water with 0.1% formic acid (A) and MS-grade methanol with 0.1% formic acid (B), which were optimized using a gradient technique at a flow rate of 0.3 mL/min. A full MS/dd-MS2 acquisition mode with positive and negative ionization was performed for untargeted metabolomics screening. Scanning ranged from 66.7-1000 m/z, with a resolution of 70,000 for full MS and 17,500 for dd-MS2. XCalibur 4.4 software (Thermo Scientific, Bremen, Germany) was used for system control.

The raw Total Ion Chromatogram (TIC) data from the metabolomics analysis were processed to identify metabolites in inhibitory and non-inhibitory root exudates. Compound Discoverer® software (Thermo Scientific, USA) was used to perform the untargeted metabolomics workflow. All raw data, including blanks (methanol), were analyzed. The results were filtered based on name, best match to MzCloud, and MS2 DDA for preferred ions.

Principal Component Analysis (PCA) and Partial Least Squares Discriminant Analysis (PLS-DA) were conducted to distinguish and classify inhibitory and non-inhibitory exudates. PERMANOVA (Permutational Multivariate Analysis of Variance) was performed using the Bray-Curtis distance matrix to assess differences between PCA groups statistically. Hierarchical clustering was performed to group the samples and metabolites based on their relative abundances, using Euclidean distance as the metric and the Ward method for linkage. A Student's t-test with FDR adjustment was used to assess the significance of normalized peak areas for each compound group. Metabolites with a PLS-DA VIP >1 and an FDR-adjusted p-value<0.05 (Xu et al. 2024) were identified as differential metabolites. Metabolomic data analysis was performed using MetaboAnalyst 6.0 (Pang et al. 2024).

RESULTS AND DISCUSSION

Antifungal effect of root exudate on *Ganoderma boninense* growth

The in vitro testing of 19 turmeric plant samples, categorized into four ecotypes, revealed a fascinating variability in the inhibitory effects. Most turmeric ecotypes produced root exudates that inhibited the colony growth of *G. boninense*. The average growth inhibition across a concentration range of 1.25-20% varied from 0.1-35.7%, with maximum inhibition ranging from 5.3-46.7%. None of the turmeric exudates at concentrations ranging from 1.25% to 20% were found to promote the growth of *G. boninense*. The inhibitory effect of the root exudates against *G. boninense* varied significantly depending on turmeric ecotypes. All five root exudates from the Palembang ecotype (Kp) exhibited the strongest antifungal activity (Figure 1), with maximum inhibition ranging from 37.7% to 46.7%. Root exudates from the Bandung (Bd) and Surabaya (Ks) ecotypes showed moderate but similar inhibitory effects (Figure 1), with inhibition ranges of 19.4%-36.2% and 10.3%-32.2%, respectively. In contrast, exudates from the Bangka ecotype (Bn) displayed weak inhibition (Figure 1), with no significant growth-suppressing effect observed (Figure 2.D).

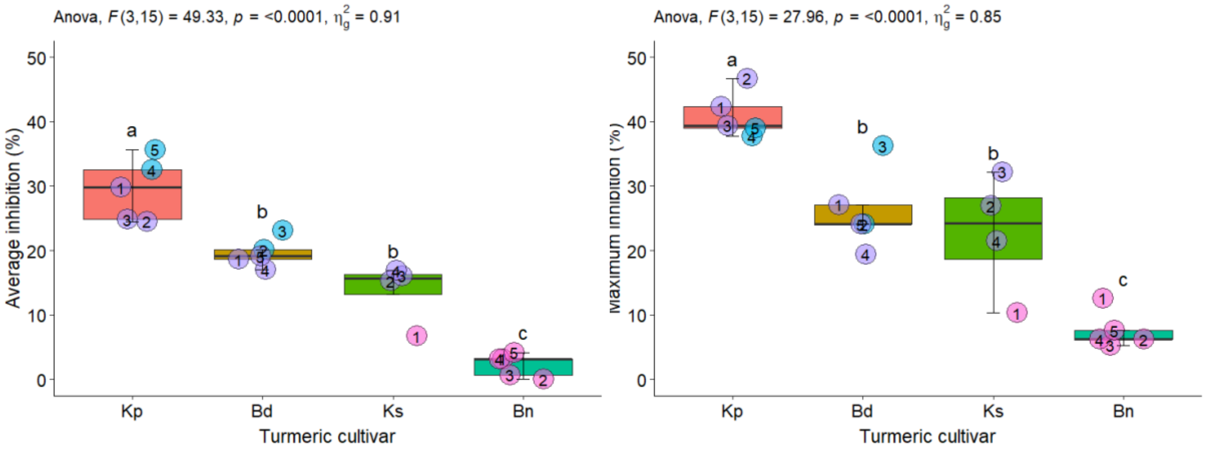

Figure 1. Average (left) and maximum (right) growth inhibition of *Ganoderma boninense* colonies on MEA medium supplemented with turmeric root exudates (1.25-20% concentration). Data points labeled in blue represent samples selected as Inhibitory Exudates (IE), and those labeled in pink represent Non-Inhibitory Exudates (NIE) for subsequent metabolomic analysis. Boxplots annotated with different letters indicate significant differences among turmeric cultivars based on HSD test

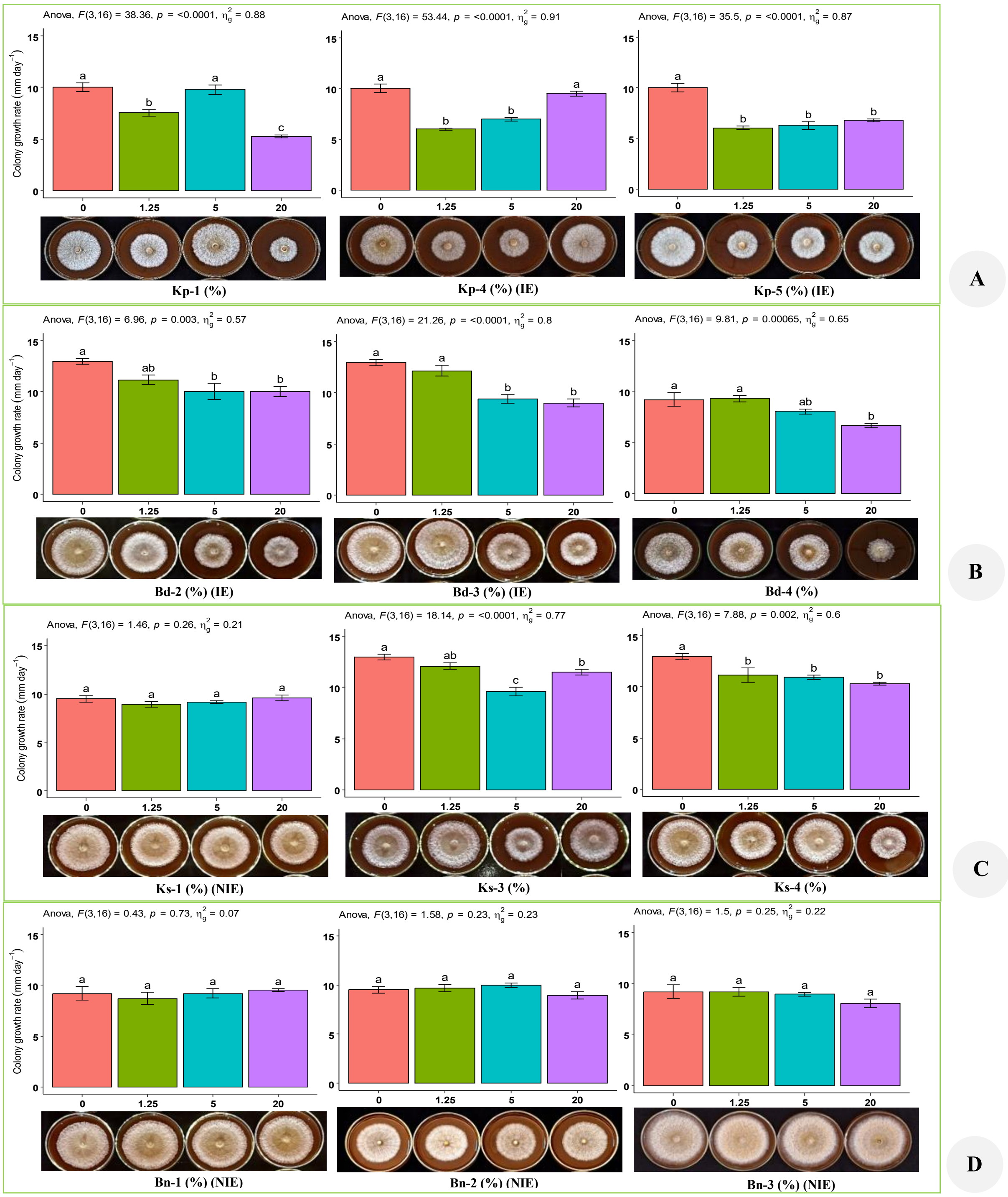

Figure 2. Colony growth of *Ganoderma boninense* on MEA medium supplemented with representative root exudates from turmeric plants of: A. Palembang (Kp), B. Bandung (Bd), C. Surabaya (Ks), and D. Bangka (Bn) ecotypes. Samples labeled with IE represent inhibitory exudates selected for metabolomic analysis, while those labeled with NIE indicate non-inhibitory exudates. Error bars represent the Standard Error of the Mean (SEM). Bars with different letters indicate significant differences among exudate concentrations according to the HSD test

The inhibitory effects were found to be concentration-dependent in certain cases. For instance, the root exudate Kp-1 (Palembang) inhibited *G. boninense* only at 1.25% and 20%, while Kp-4 was effective between 1.25% and 5%. In contrast, Kp-5 exhibited consistent inhibition across all tested concentrations (1.25%-20%) (Figure 2.A). The exudates from Bandung (Bd) generally inhibited fungal growth more consistently at higher concentrations (5-20%), with less variation among samples (Figure 2.B). Root exudates from the Surabaya ecotype (Ks) showed more variability. One sample (Ks-1) did not produce a significant inhibitory effect, while the other three samples demonstrated similar levels of inhibition (Figure 2.C). Increasing the exudate concentration did not consistently enhance inhibitory activity, particularly for the Palembang (Kp) and Surabaya (Ks) ecotypes. In contrast, a concentration-dependent increase in inhibition was evident in exudates from Bandung (Bd), particularly between 1.25% and 5% (Figure 2). The suppression of *G. boninense* colony growth by turmeric root exudates was irreversible. Even after transferring the fungal colonies to an exudate-free medium, mycelial growth remained suppressed. This suggests a fungicidal rather than fungistatic mode of action.

Metabolomic study of root exudate

An untargeted metabolomic analysis using LC-HRMS identified 193 distinct metabolites in turmeric root exudates. These metabolites encompassed a wide range of compounds classified into 36 chemical classes, predominantly including lipids (fatty acyls, prenol lipids, steroids, glycerolipids, and glycerophospholipids), as well as organooxygen compounds, benzene derivatives, carboxylic acids, and various secondary metabolites (Figure 3.A). A total of 72 metabolites from group IE, 70 from group NIE, and 51 shared metabolites between the two groups were selected and submitted to MetaboAnalyst 6.0. The data were analyzed using Principal Component Analysis (PCA) to evaluate the metabolic differences between the inhibitory and non-inhibitory exudate groups. Samples from each group formed distinct clusters, with the IE group clustering closely and the NIE group forming a separate branch. Principal components PC1 and PC2 accounted for 58.5% of the total variation, clearly differentiating the IE and NIE groups and indicating significant metabolic differences (PERMANOVA, p-value = 0.005) (Figure 3.B).

Hierarchical clustering revealed distinct groupings of samples and metabolites based on their relative abundance, highlighting unique metabolic profiles that differentiate the IE and NIE groups. Notably, most metabolites were more abundant in the IE group, indicating a complex composition of the *Ganoderma* growth-inhibitory exudate. In contrast, the NIE group exhibited a lower abundance of these metabolites (Figure 4).

In total, 34 metabolites showed significant differences between the two groups (FDR-adjusted p-value<0.05). Of these, 25 were upregulated in the IE group, and nine were upregulated in the NIE group. Twenty-seven metabolites with PLS-DA VIP scores above 1.0 were identified as differential metabolites. Notably, 20 of these—including nootkatone, phthalic anhydride, oxidized latia luciferin, 2,6-dimethylquinoline, (+/-)9,10-dihydroxy-12Z-octadecenoic acid, 10,16-dihydroxyhexadecanoic acid, 3R-[3R-(3R-Hydroxybutyryloxy)-butyryloxy]buteric acid, 3,6-nonadienal, dodecanamide, bis(2-ethylhexyl) phthalate, 2R-aminohexadecanoic acid, 6-methylquinoline, 2-dodecylbenzenesulfonic acid, lehualide I, azelaic acid, haplofungin C, dichotellate A, piptamine, (-)-menthyl acetate, and beta-estradiol—were significantly expressed in the IE group. Nootkatone, phthalic anhydride, and oxidized latia luciferin were the most differential metabolites with the highest PLS-DA VIP scores and abundance in the inhibitory compared to the non-inhibitory exudate. However, seven metabolites, including pentaethylene glycol, microdiplactone, 6,8-dihydroxy-octanoic acid, 4E,6E,10Z-hexadecatrien-1-ol, PGE2alpha dimethyl amine, asenjonamide B, and tridodecylamine, were significantly abundant in the NIE group (Figure 5).

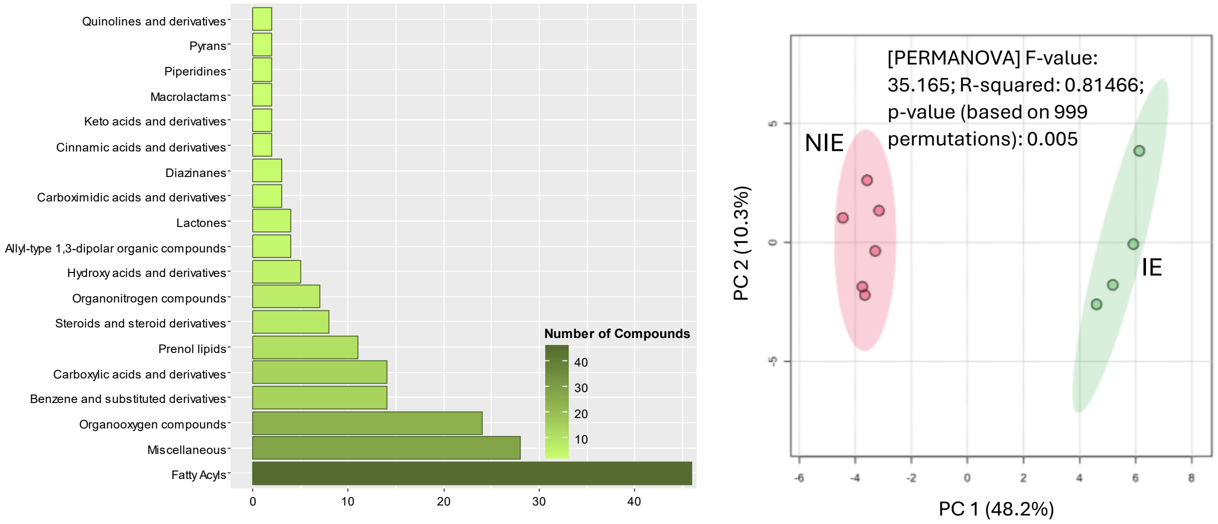

A **B**

Figure 3. A. Histogram of the number of LC-HRMS annotated substances by chemical class, B. PCA score plot grouped the substances of *Ganoderma* growth-Inhibitory Exudate (IE) and Non-Inhibitory Exudate (NIE) of turmeric root exudate

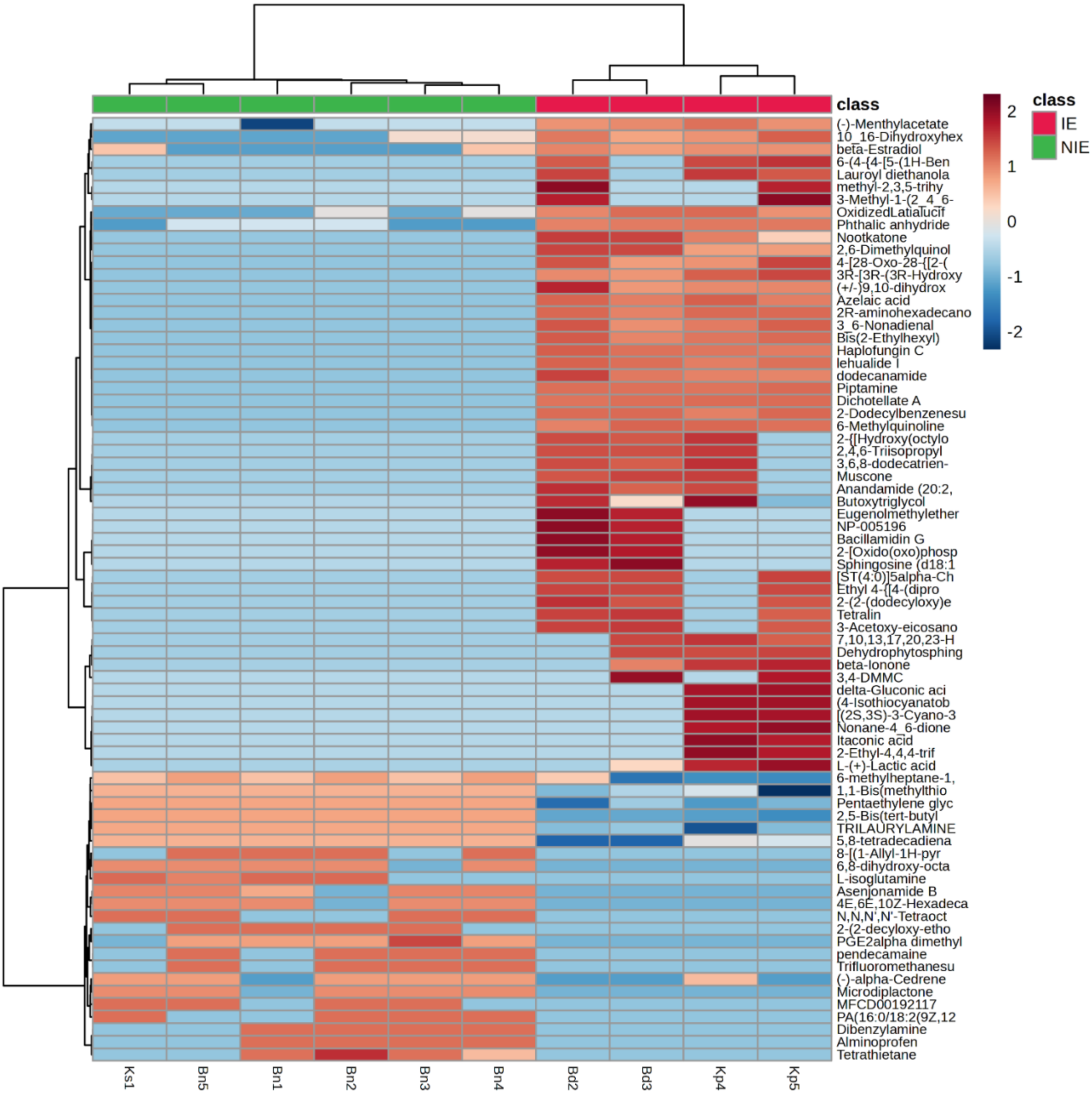

Figure 4. The heatmap profile illustrates the relative abundance of the top 75 most abundant metabolites in turmeric root exudates, comparing those with growth inhibition against *Ganoderma boninense* (IE group) to those without growth inhibition (NIE group). The color scale represents metabolite abundance, ranging from dark blue (low abundance) to dark red (high abundance). Individual samples corresponding to each column are labeled at the bottom of the figure

Discussion

This study found that crude, unprocessed root exudates from different turmeric ecotypes exhibit antifungal activity against *G. boninense*, the causative agent of basal stem rot in oil palm. The antifungal effect was concentration-dependent and varied according to the ecotype. Thus far, there have been no studies exploring the use of root exudates from rhizomatous plants for disease control. However, antifungal root exudates have been reported in other resistant or invasive plant species, exhibiting antifungal activity comparable to that of turmeric root exudates. For instance, root exudates from a tobacco variety known for *Phytophthora* resistance (Gexin 3) contain higher levels of tartaric, ferulic, and lauric acids, which have been shown to reduce mycelial growth (30-46%) and inhibit spore germination (25-40%) of *P. nicotianae* (Zhang et al. 2020). Moreover, Peng et al. (2024) observed that root exudates from another resistant tobacco strain (K326) hindered *P. nicotianae* colony growth by 15%, with isoliquiritigenin and lauric acid identified as key antifungal compounds. The organic phase of wheat root exudates inhibited *Fusarium oxysporum* colony proliferation by 1.4-49.3%, with phytosphingosine, the principal allelochemical compound, exhibiting inhibition rates of 12.3-29.3% (Li et al. 2020). Root exudates from the legumes *Desmodium uncinatum* and *Mucuna pruriens*, which contain phenolic acids (benzoic, *trans*-cinnamic, *p*-coumaric, and *p*-hydroxybenzoic), suppressed mycelial growth of *Fusarium oxysporum* f. sp. *cubense* by 72-74% (Were et al. 2022). In addition, root exudates from the invasive plant *Wedelia trilobata* exhibited antifungal activity against various soil-borne pathogens, including *Rhizoctonia solani*, *Sclerotinia sclerotiorum*, and *Fusarium oxysporum*, with fungal growth inhibition ranging from 2.30-36.32% (Xiang et al. 2023).

The untargeted LC-HRMS metabolomics analysis identified 193 distinct metabolites, predominantly lipids, in turmeric root exudates. *Ganoderma* growth-inhibitory exudates have a greater abundance of metabolites, particularly 20 differential metabolites, showing the complex metabolites involved in the inhibitory effect. Three of the most differential metabolites—nootkatone, phthalic anhydride, and oxidized latia luciferin—were not known to have inherent antifungal properties. Nootkatone, a natural sesquiterpene, has been reported to exhibit antibacterial activities against Gram-positive bacteria such as *Staphylococcus aureus*, *Enterococcus faecalis*, *Listeria monocytogenes*, *Corynebacterium diphtheriae*, and *Bacillus cereus* (Yamaguchi 2019). Nootkatone has been proven to inhibit the growth of bacteria like *S. aureus* and can even prevent the formation of biofilms, inhibit the swarming motility, disrupt the preformed biofilms, and eradicate the bacteria within biofilms (Farha et al. 2020).

Five of the remaining 17 differential metabolites—azelaic acid, bis(2-ethylhexyl) phthalate, haplofungin C, menthyl acetate, and piptamine—are known to have antifungal properties. Azelaic acid, a naturally occurring dicarboxylic fatty acid produced by microorganisms and plants, is a well-established antibacterial and exhibits activity against dermatophytes such as *Scopulariopsis brevicaulis*, *Candida glabrata*, and *Pityrosporum ovale* (Spaggiari et al. 2023). Bis(2-ethylhexyl) phthalate is an ester of phthalic acid, commonly used as a plasticizer; it is naturally produced by plants or microorganisms such as bacteria or fungi (Ortiz and Sansinenea 2018). Bis(2-ethylhexyl) phthalate was isolated from the River Nile-derived fungus *Aspergillus awamori*, showing antifungal activity against *Candida albicans* (Lotfy et al. 2018). Additionally, Bis(2-ethylhexyl) phthalate has been identified as a key compound in the metabolite profile of culture filtrates of bacterial from straw mushrooms with antifungal effects against *Cercospora lactucae*, *Colletotrichum gloeosporioides*, and *Fusarium oxysporum* f.sp. *cubense* (Masrukhin et al. 2021). Bis(2-ethylhexyl) phthalate has been detected as a key compound in the metabolite profile of endophytic bacteria *Bacillus amyloliquefaciens* and *Bacillus velezensis* with antifungal properties against *Alternaria* and *Helminthosporium* (Soliman et al. 2022b).

Haplofungin C, isolated from a culture broth of the fungus strain *Lauriomyces bellulus*, exhibited antifungal activity against *Candida glabrata* (Ohnuki et al. 2009). Haplofungin, a compound derived from microbes, inhibits fungal inositol phosphorylceramide synthase, with low nano-molar IC_{50} values against *Saccharomyces cerevisiae* (Pinneh et al. 2019). Menthyl acetate is a major compound in *Mentha longifolia* essential oils that exhibits antifungal properties against *Fusarium oxysporum*, a root rot pathogen of tomato (Soliman et al. 2022a).

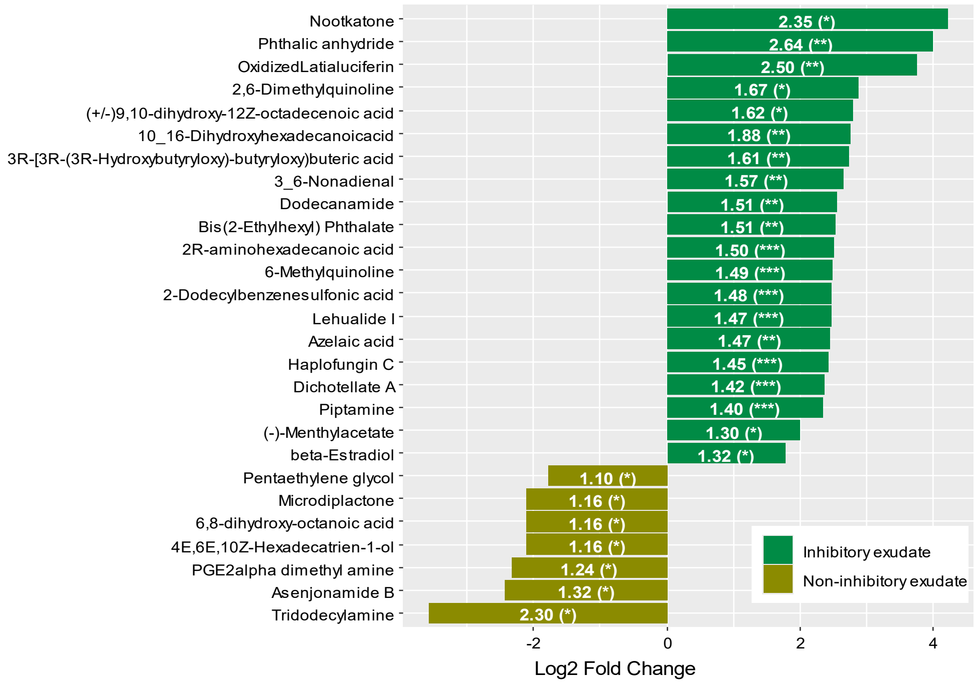

Figure 5. Differential metabolite analysis of *Ganoderma*-inhibitory and non-inhibitory turmeric root exudates based on Log2(Fold Change), PLS-DA VIP>1.0 (values within each bar), and FDR-adjusted p-value (*p<0.05, **p<0.01, ***p<0.001)

Piptamine is an antibiotic aromatic amine compound isolated from the fungus *Piptoporus betulinus*, which has demonstrated antimicrobial activity against bacteria and certain fungi, including *Kluyveromyces marxianus*, *Candida albicans*, *Sporobolomyces salmonicolor*, and *Rhodotorula rubra* (Li et al. 2024). Piptamine is also detected as a major compound in the crude culture filtrate of the endophytic fungus *Pseudopithomyces chartarum*, showing antimicrobial activity in protecting the forage crop *Lupinus luteus* against *Phytophthora cinnamomi* (García-Latorre et al. 2024). The metabolomic study indicated that the observed antifungal effects of turmeric root exudate resulted from the synergistic interaction of multiple known antifungal compounds produced by turmeric root exudate.

Turmeric rhizome extracts have been widely studied for their antimicrobial properties. Various antifungal compounds, including curcuminoids, terpenoids, and other phytochemicals, have been isolated from these extracts and shown to inhibit a broad spectrum of fungi, including those classified under the classes Sordariomycetes, Zygomycetes, Dothideomycetes, Leotiomycetes, Hyphomycetes, and Eurotiomycetes (Akter et al. 2018, 2019; Chen et al. 2018). However, despite the presence of these potent antifungal compounds in the rhizome, they have not been detected in root exudates. None of the five differential metabolites with known antifungal properties had been reported as putative metabolites of turmeric plants. Research on the biological properties of turmeric root exudates remains limited. Our previous study provided preliminary evidence of the antimicrobial activity of turmeric root exudates, which reduced wood colonization by *G. boninense* mycelium (Rahmadhani et al. 2018). These findings suggest that turmeric root exudates may contain unique and previously uncharacterized bioactive compounds with potential antifungal applications.

Antifungal compounds may be found in turmeric root exudates due to the interactions between beneficial microbial communities from the compost extract fertilizer and the plant roots. The compost extract used in this study contained diverse microbial populations, dominated by phosphate-solubilizing, chitinolytic, and cellulolytic *Lactobacillus* and *Saccharomyces* (Suwandi et al. 2020) that could have influenced the composition of root exudates by inducing plant metabolic responses. The presence of these microbial interactions may have contributed to the production of root exudate metabolites with antifungal properties. Other studies have demonstrated that microbial colonization can significantly alter root exudate composition, particularly by inducing the production of lipid-related metabolites and defense compounds, which are crucial in plant immunity and pathogen suppression (Fracchia et al. 2024). Enhancing the antifungal activity of turmeric root exudates through the colonization of beneficial microbial communities offers a promising strategy for developing eco-friendly biocontrol agents against *G. boninense* in oil palm plantations.

Turmeric root exudates did not promote the growth of *G. boninense* even at a high concentration of 20%, indicating their potential suitability as a biocontrol agent. This contrasts with the root exudates of *Panax ginseng,* which, at high concentrations, have been reported to stimulate the growth of pathogenic fungi such as *Fusarium* while simultaneously suppressing beneficial microbes like *Mortierella*. Additionally, elevated concentrations of root exudates from *P. ginseng* and other *Panax* species have shown allelopathic autotoxicity effects (Sun et al. 2023). Although specific data on the direct effects of turmeric root exudates on oil palm or other crops are limited, observations from intercropping systems offer insight. In our previous study (unpublished), intercropping turmeric with oil palm seedlings did not result in growth inhibition. Similarly, detrimental effects on immature oil palm were not reported in plantations employing turmeric intercropping (Dissanayake and Palihakkara 2024). Furthermore, when intercropped with patchouli (*Pogostemon cablin*), turmeric enhanced soil microbial abundance, diversity, and community structure, suggesting a positive ecological role of its root exudates (Zeng et al. 2020).

In conclusion, these findings indicate that root exudates from turmeric plants grown in soil amended with fermented compost extract exhibit antifungal properties against *G. boninense*, the causative agent of basal stem rot in oil palm. The local Palembang ecotype showed the highest inhibitory effect, reducing fungal growth by up to 47%. Metabolomic profiling revealed 193 metabolites, of which five—azelaic acid, bis(2-ethylhexyl) phthalate, haplofungin C, menthyl acetate, and piptamine—were significantly enriched in the inhibitory exudate group and are presumed to contribute to antifungal activity. The inhibitory exudates also contained high levels of nootkatone, a potent antibacterial compound active against Gram-positive bacteria. These findings not only provide a foundation for developing biocontrol strategies against plant diseases but also inspire hope and excitement for the future of plant disease management.

ACKNOWLEDGEMENTS

This work was financially supported by a Fundamental Research Grant (090/E5/PG.02.00.PL/2024 and 0015.027/UN9/SB1.LP2M.PT/2024) from the Directorate for Research and Community Service, Ministry of Culture, Research and Technology, the Republic of Indonesia.

REFERENCES

Akter J, Hossain MA, Sano A, Takara K, Islam MZ, Hou D-X. 2018. Antifungal activity of various species and strains of turmeric (*Curcuma* spp.) against (*Fusarium solani*) sensu lato. Pharm Chem J 52: 320-325. DOI: 10.1007/s11094-018-1815-4.

Akter J, Islam MZ, Takara K, Hossain MA, Sano A. 2019. Isolation and structural elucidation of antifungal compounds from Ryudai gold (*Curcuma longa*) against *Fusarium solani* sensu lato isolated from American manatee. Comp Biochem Physiol C Toxicol Pharmacol 219: 87-94. DOI: 10.1016/j.cbpc.2019.02.011.

Chen C, Long L, Zhang F, Chen Q, Chen C, Yu X, Liu Q, Bao J, Long Z. 2018. Antifungal activity, main active components and mechanism of *Curcuma longa* extract against *Fusarium graminearum*. PLoS One 13 (3): e0194284. DOI: 10.1371/journal.pone.0194284.

de Souza LP, Alseekh S, Scossa F, Fernie AR. 2021. Ultra-high-performance liquid chromatography high-resolution mass spectrometry variants for metabolomics research. Nat Methods 18: 733-746. DOI: 10.1038/s41592-021-01116-4.

Dissanayake SM, Palihakkara IR. 2024. Effects of intercropping of immature oil palm (*Elaeis guineensis*) with banana, ginger, and turmeric in the Galle District, Sri Lanka. Environ Qual Manag 33 (4): 31-36. DOI: 10.1002/tqem.21980.

Farha AK, Yang Q-Q, Kim G, Zhang D, Mavumengwana V, Habimana O, Li H-B, Corke H, Gan R-Y. 2020. Inhibition of multidrug-resistant foodborne *Staphylococcus aureus* biofilms by a natural terpenoid (+)-nootkatone and related molecular mechanism. Food Control 112: 107154. DOI: 10.1016/j.foodcont.2020.107154.

Fracchia F, Guinet F, Engle NL, Tschaplinski TJ, Veneault-Fourrey C, Deveau A. 2024. Microbial colonisation rewires the composition and content of poplar root exudates, root and shoot metabolomes. Microbiome 12 (1): 173. DOI: 10.1186/s40168-024-01888-9.

García-Latorre C, Rodrigo S, Santamaria O. 2024. Evaluation of the extract of *Pseudopithomyces chartarum* to be used as biocontrol agent against *Phytophthora cinnamomic* in *Lupinus luteus*. J Soil Sci Plant Nutr 24: 6325-6337. DOI: 10.1007/s42729-024-01969-6.

Gu M, Jin J, Lu P, Yu S, Su H, Shang H, Yang Z, Zhang J, Cao P, Tao J. 2024. Regulation of root-associated microbiomes and root exudates by different tobacco species. Chem Biol Technol Agric 11: 151. DOI: 10.1186/s40538-024-00678-7.

Hussien AM, Abbas MS. 2023. Effect of allelopathic potential of some plants root exudates concerning growth and pathogenicity of some fungus on *Brassica oleracea* varplant. IOP Conf Ser: Earth Environ Sci 1158: 072006. DOI: 10.1088/1755-1315/1158/7/072006.

Ibrahim MS, Seman IA, Rusli MH, Izzuddin MA, Kamarudin N, Hashim K, Abd Manaf Z. 2020. Surveillance of *Ganoderma* disease in oil palm planted by participants of the smallholders replanting incentive scheme in Malaysia. J Oil Palm Res 32 (2): 237-244. DOI: 10.21894/jopr.2020.0024.

Kamu A, Phin CK, Seman IA, Gabda D, Mun HC. 2021. Estimating the yield loss of oil palm due to *Ganoderma* basal stem rot disease by using Bayesian model averaging. J Oil Palm Res 33 (1): 46-55. DOI: 10.21894/jopr.2020.0061.

Khoo YW, Chong KP. 2023. *Ganoderma boninense*: General characteristics of pathogenicity and methods of control. Front Plant Sci 14: 1156869. DOI: 10.3389/fpls.2023.1156869.

Li C, Tian Q, u Rahman MK, Wu F. 2020. Effect of antifungal compound phytosphingosine in wheat root exudates on the rhizosphere soil microbial community of watermelon. Plant Soil 456: 223-240. DOI: 10.1007/s11104-020-04702-1.

Li J, Li Z, Duan Y, Liu C, Yan M. 2024. Secondary metabolites of *Fomitopsis betulina*: Chemical structures, biological activity and application prospects. J Fungi 10 (9): 616. DOI: 10.3390/jof10090616.

Lima GS, Lima NM, Roque JV, de Aguiar DVA, Oliveira JVA, dos Santos GF, Chaves AR, Vaz BG. 2022. LC-HRMS/MS-based metabolomics approaches applied to the detection of antifungal compounds and a metabolic dynamic assessment of Orchidaceae. Molecules 27 (22): 7937. DOI: 10.3390/molecules27227937.

Lotfy MM, Hassan HM, Hetta MH, El-Gendy AO, Mohammed R. 2018. Di-(2-ethylhexyl) phthalate, a major bioactive metabolite with antimicrobial and cytotoxic activity isolated from River Nile derived fungus *Aspergillus awamori*. Beni Suef Univ J Basic Appl Sci 7 (3): 263-269. DOI: 10.1016/j.bjbas.2018.02.002.

Masrukhin M, Putri AL, Sulistiyani TR, Ilyas M, Purnaningsih I, Saskiawan I, Niam MY. 2021. Antifungal activity of bacterial isolates from straw mushroom cultivation medium against phytopathogenic fungi. J Trop Biodivers Biotechnol 6 (1): jtbb59235. DOI: 10.22146/jtbb.59235.

Ohnuki T, Yano T, Ono Y, Kozuma S, Suzuki T, Ogawa Y, Takatsu T. 2009. Haplofungins, novel inositol phosphorylceramide synthase inhibitors, from *Lauriomyces bellulus* SANK 26899 I. Taxonomy, fermentation, isolation and biological activities. J Antibiot 62 (10): 545-549. DOI: 10.1038/ja.2009.72.

Ortiz A, Sansinenea E. 2018. Di-2-ethylhexylphthalate may be a natural product, rather than a pollutant. J Chem 2018 (1): 6040814. DOI: 10.1155/2018/6040814.

Pang Z, Lu Y, Zhou G, Hui F, Xu L, Viau C, Spigelman AF, MacDonald PE, Wishart DS, Li S, Xia J. 2024. MetaboAnalyst 6.0: Towards a unified platform for metabolomics data processing, analysis and interpretation. Nucleic Acids Res 52 (W1): W398-W406. DOI: 10.1093/nar/gkae253.

Peng S, Shu F, Lu Y, Fan D, Zheng D, Yuan G. 2024. Quasi-targeted metabolomics revealed isoliquiritigenin and lauric acid associated with resistance to tobacco black shank. Plant Signal Behav 19 (1): 2332019. DOI: 10.1080/15592324.2024.2332019.

Pinneh EC, Mina JG, Stark MJR, Lindell SD, Luemmen P, Knight MR, Steel PG, Denny PW. 2019. The identification of small molecule inhibitors of the plant inositol phosphorylceramide synthase which demonstrate herbicidal activity. Sci Rep 9 (1): 8083. DOI: 10.1038/s41598-019-44544-1.

Priwiratama H, Prasetyo AE, Susanto A. 2020. Incidence of basal stem rot disease of oil palm in converted planting areas and control treatments. IOP Conf Ser: Earth Environ Sci 468: 012036. DOI: 10.1088/1755-1315/468/1/012036.

Rahmadhani TP, Suwandi S, Pujiastuti Y. 2018. Growth response of *Ganoderma* sp. mycelium treated with root exudates of herbaceous plants. Biovalentia: Biol Res J 4: 28-31. DOI: 10.24233/biov.4.1.2018.88.

Salem MA, Wang JY, Al-Babili S. 2022. Metabolomics of plant root exudates: From sample preparation to data analysis. Front Plant Sci 13: 1062982. DOI: 10.3389/fpls.2022.1062982.

Soliman SA, Hafez EE, Al-Kolaibe AMG, Abdel Razik E-SS, Abd-Ellatif S, Ibrahim AA, Kabeil SSA, Elshafie HS. 2022a. Biochemical characterization, antifungal activity, and relative gene expression of two mentha essential oils controlling *Fusarium oxysporum*, the causal agent of *Lycopersicon esculentum* root rot. Plants 11:189. DOI: 10.3390/plants11020189.

Soliman SA, Khaleil MM, Metwally RA. 2022b. Evaluation of the antifungal activity of *Bacillus amyloliquefaciens* and *B. velezensis* and characterization of the bioactive secondary metabolites produced against plant pathogenic fungi. Biology 11 (10): 1390. DOI: 10.3390/biology11101390.

Spaggiari C, Annunziato G, Spadini C, Montanaro SL, Iannarelli M, Cabassi CS, Costantino G. 2023. Extraction and quantification of azelaic acid from different wheat samples (*Triticum durum* Desf.) and evaluation of their antimicrobial and antioxidant activities. Molecules 28 (5): 2134. DOI: 10.3390/molecules28052134.

Sun J, Yang J, Zhao S, Yu Q, Weng L, Xiao C. 2023. Root exudates influence rhizosphere fungi and thereby synergistically regulate *Panax ginseng* yield and quality. Front Microbiol 14: 1194224. DOI: 10.3389/fmicb.2023.1194224.

Suwandi S, Alesia M, Munandar RP, Fadli R, Suparman S, Irsan C, Muslim A. 2024. The suppression of *Ganoderma boninense* on oil palm under mixed planting with taro plants. Biodiversitas 25 (3): 1143-1150. DOI: 10.13057/biodiv/d250329.

Suwandi S, Irsan C, Muslim A, Herlinda S. 2020. Protection of chili pepper from mosaic virus disease and *Aphis gossypii* by a fermented water extract of compost. IOP Conf Ser: Earth Environ Sci 468: 012043. DOI: 10.1088/1755-1315/468/1/012043.

Suwandi S, Munandar RP, Suparman S, Irsan C, Muslim A. 2023. Mixed planting with rhizomatous plants interferes with *Ganoderma* disease in oil palm. J Oil Palm Res 35: 354-364. DOI: 10.21894/jopr.2022.0043.

Suwandi S, Rahmadhani TP, Suparman S, Irsan C, Muslim A. 2022. Allelopathic potential of root exudates from perennial herbaceous plants against *Ganoderma boninense*. IOP Conf Ser: Earth Environ Sci 976: 012053. DOI: 10.1088/1755-1315/976/1/012053.

Triastuti A, Vansteelandt M, Barakat F, Amasifuen C, Jargeat P, Haddad M. 2023. Untargeted metabolomics to evaluate antifungal mechanism: A study of *Cophinforma mamane* and *Candida albicans* interaction. Nat Prod Bioprospect 13 (1): 1. DOI: 10.1007/s13659-022-00365-w.

Upasani ML, Gurjar GS, Kadoo NY, Gupta VS. 2016. Dynamics of colonization and expression of pathogenicity related genes in *Fusarium oxysporum* f.sp. *ciceri* during chickpea vascular wilt disease progression. PLoS One 11 (5): e0156490. DOI: 10.1371/journal.pone.0156490.

Virdiana I, Forster BP, Zakaria L. 2024. Basal stem rot of oil palm: Disease development in mineral and peat soils. IOP Conf Ser: Earth Environ Sci 1308: 012025. DOI: 10.1088/1755-1315/1308/1/012025.

Were E, Schöne J, Viljoen A, Rasche F. 2022. Phenolics mediate suppression of *Fusarium oxysporum* f. sp. *cubense* TR4 by legume root exudates. Rhizosphere 21: 100459. DOI: 10.1016/j.rhisph.2021.100459.

Wu J, Zhou J, Yang C, Kuang Y, Qi C, Guo F, Zhao Q. 2025. The composition of root exudates between resistant and susceptible konjac species against soft rot disease. J Plant Dis Prot 132: 83. DOI: 10.1007/s41348-025-01073-6.

Xiang Y, Javed Q, Wu Y, Bo Y, Dai Z, Huang P, Sun J, Du D. 2023. Root exudates of *Wedelia trilobata* suppress soil-borne pathogenic fungi and increase its invasion. Pol J Environ Stud 32 (5): 4865-4875. DOI: 10.15244/pjoes/168421.

Xu S, Bai C, Chen Y, Yu L, Wu W, Hu K. 2024. Comparing univariate filtration preceding and succeeding PLS-DA analysis on the differential variables/metabolites identified from untargeted LC-MS metabolomics data. Anal Chim Acta 1287: 342103. DOI: 10.1016/j.aca.2023.342103.

Yamaguchi T. 2019. Antibacterial properties of nootkatone against gram-positive bacteria. Nat Prod Commun 14 (6): 1-5. DOI: 10.1177/1934578X19859999.

Zakaria L. 2023. Basal stem rot of oil palm: The pathogen, disease incidence, and control methods. Plant Dis 107 (3): 603-615. DOI: 10.1094/pdis-02-22-0358-fe.

Zeng J, Liu J, Lu C, Ou X, Luo K, Li C, He M, Zhang H, Yan H. 2020. Intercropping with turmeric or ginger reduce the continuous cropping obstacles that affect *Pogostemon cablin* (patchouli). Front Microbiol 11: 579719. DOI: 10.3389/fmicb.2020.579719.

Zhang C, Feng C, Zheng Y, Wang J, Wang F. 2020. Root exudates metabolic profiling suggests distinct defense mechanisms between resistant and susceptible tobacco cultivars against black shank disease. Front Plant Sci 11: 559775. DOI: 10.3389/fpls.2020.559775.